MAGNETIC COFFEE RESIDUE BIOSORBENT FOR SELECTIVE EXTRACTION OF ZINC OXIDE NANOPARTICLES IN WATER SAMPLES

Yasmin Abdurahman[1], Deribachew Bekana[1], Ayalew Temesgen[1], Negussie Bussa[2], Minbale Aschale[3], Endale Teju[1] and Meseret Amde[1*]

[1]Department of Chemistry, College of Natural and Computational Sciences, Haramaya University, Haramaya, Ethiopia
[2]Department of Food Science and Post-Harvest Technology, Haramaya Institute of Technology, Haramaya University, Haramaya, Ethiopia
[3]Technology and Innovation Institute of Ethiopia, Addis Ababa, Ethiopia

ABSTRACT. Quantification of engineered nanomaterials in the environment has attracted researchers' interest recently because of their increased release to the environment. In this study, a recyclable and easily accessible magnetized coffee residue (MCR) is proposed for magnetic solid-phase extraction (MSPE) of zinc oxide nanoparticles (ZnO-NPs) from water samples. The MCR was synthesized using a simple one-step chemical co-precipitation method from coffee residue and was characterized by state-of-the-art techniques. Various parameters affecting the MSPE efficiency of ZnO-NPs were optimized and 8.5 pH, 75 mg adsorbent, 120 min extraction time, 10 mL sample volume, 4 mL of 0.001 M HCl as an eluting solvent, and 30 min elution time were identified as the optimum conditions. Under these conditions, the method showed excellent linearity (R^2 = 0.995) and good sensitivity (detection limit, 0.12 mg L^{-1}, and quantification limit, 0.4 mg L^{-1}). Intra and inter-day percent standard deviations were 1.4 and 2.2%, respectively, for the analysis of 6 mg L^{-1} ZnO-NPs. The practical applicability of the method for the extraction of ZnO-NPs in environmental samples was evaluated, and recovery values in the range of 93.0–98.2% were obtained, confirming its successful performance. Generally, the technique is easy, economical, and eco-friendly that can be considered for the extraction of metal oxide nanoparticles.

KEY WORDS: Zinc oxide nanoparticles, Magnetic coffee residue, Magnetic solid-phase extraction, Flame atomic absorption spectroscopy, Environmental waters

INTRODUCTION

Metal oxide nanoparticles (NPs) are categorized as engineered nanomaterials that are widely known recently, and among them, zinc oxide nanoparticles (ZnO-NPs) are extensively produced, about 100 to 1000 tons year^{-1}, within the world [1]. Because it is a well-known semiconductor [2] due to its outstanding properties like wide bandgap (3.37 eV), high exciting binding energy (60 mV), high dielectric constant, and high optoelectronic efficiencies relative to the indirect bandgap, it has been used in areas like photocatalysis, chemical remediation, environmental analysis, photoinitiation of polymerization reactions, quantum dot devices, alternative energy conversion, biochemical sensors, chemical electrode, cosmetics, and pigments [3-9]. ZnO-NPs has also good biocompatibility with human cells [10]. On the other hand, it has been applied for antibacterial and antifungal activities [11, 12]. These reports affirm that the discharge of ZnO-NPs to the environment is obvious and requires cautious monitoring. On the opposite hand, metal oxide NPs may exhibit significant toxic effects due to their inherent toxic properties [13, 14] and their deleterious effects could be enhanced due to their transformation products in environmental systems [15]. Hence, the discharge of ZnO-NPs into the water body may cause pollution and has become a burning issue. Therefore, to understand the toxicity and fate of the supplies within the environmental systems, and to precisely describe its effects, the concentration of the NPs should be determined [16].

_____

Hitherto, few methods are proposed to extract, separate and preconcentrate ZnO-NPs from waters [17]. Cloud point extraction-based technique was used for the examination of ZnO-NPs during which the NPs were extracted with Triton X-114 followed by digestion before ICP-MS determination [18, 19]. Although the report had some advancements from analytical chemistry point of view, it is tedious and time-consuming. Additionally, the use of solid-phase extraction (SPE) to extract and enrich NPs have been reported in the literature. As an example, using ionic exchange resin, a unique and selective SPE method was reported for the effective extraction of NPs from environmental water [20, 21]. On the other hand, the use of an organic solvent to desorb the extracted analyte and the long desorption time (over 3 h) can be stated as their shortcomings.

Among the wide selection of such methods, magnetic SPE (MSPE) which uses a magnetic adsorbent material has received much attention because of its great flexibility and rapidity. The MSPE is predicated on the dispersion of a magnetic adsorbent in a solution containing the target analyte followed by magnetic separation, and then redispersion in an appropriate eluent and digested to get rid of a matrix before the final instrumentation. Magnetic separations are much more suitable, inexpensive, and effective, and allow a rapid mass transfer. Consequently, MSPE is commonly used in the extraction of trace metals [22] and organic compounds [23].

Biomass obtained from agricultural and food wastes (e.g. tea leaves, rice hulls, coffee husk among others) are exploited to improve the water quality [24], and metal-binding ability of such materials might be due to the comprising polyhydroxy groups [25]. Albeit their advantages, separating the spent adsorbent from the solution phase is a difficult job and can be mentioned as one of their shortcomings. Due to this, the surfaces of those biomasses are often improved with magnetic materials which help to beat their deficiency and are simply recovered by an external magnet [26, 27]. Magnetically modified coffee dregs showed a high ability in removing particular xenobiotics, like dyes within the literature [28]. Zuorro and Lavecchia also reported the adsorption of methylene blue with a coffee residue-based magnetic biosorbents [29]. In very recently, the magnetized coffee residue was utilized for the effective TiO_2-NPs extraction prior to graphite furnace atomic absorption spectroscopic technique [30]. Unluckily, most of the magnetized coffee residue materials showed low adsorption capacities and weak stabilities which could ensue due to the synthesis route followed. This indicates a potential adsorbent with long-lasting stability and short-time recovery has to be proposed and formulated through adsorbent modification with excellent materials having strong magnetic properties like Fe_3O_4-NPs.

In this work, a homemade magnetic coffee residue (MCR) based MSPE procedure was proposed to extract and separate ZnO-NPs in environmental water before flame atomic absorption spectroscopy (FAAS). The adsorbent was prepared within the course of co-precipitation of iron(II) and iron(III) in the existence of initially processed coffee residue. The MSPE method was developed accordingly and was applied for selective extraction and efficient preconcentration of the analyte in real waters for validation studies. It is worth mentioning that MCR has not been employed as an adsorbent for the extraction of ZnO-NPs to the best of our knowledge.

EXPERIMENTAL

Chemicals and reagents

All chemicals and reagents were of analytical grade. Zinc acetate dihydrate ($Zn(CH_3COO)_2 \cdot 2H_2O$) was purchased from Sinopharm Chemical Reagent Co. Ltd., (Shanghai, China). Sodium chloride (NaCl, 99.8%), sodium hydroxide (NaOH, 98%), and acetone (98%) were obtained from Merck (Darmstadt, Germany). Ethanol (AR, 99.7%) and methanol (99.8%) were acquired from Beijing Chemical Works (Beijing, China). Sodium nitrate ($NaNO_3$, 99.5%), conc. nitric acid (69%), sulfuric acid (97–99%), and hydrochloric acid (35–38%) were obtained from Blulux laboratories Pvt. Ltd. (Faridabad, India). Hydrogen peroxide (35%) and ammonia solution (25 *wt*%) were purchased from BDH Chemicals Ltd. (Poole, England). Two hydrated iron chloride salts,

$FeCl_3 \cdot 6H_2O$ and $FeCl_2 \cdot 4H_2O$, were received from Sigma-Aldrich (St. Louis, USA). Distilled and deionized water (DDW) was used throughout the experimental work.

Preparation of ZnO-NPs

After minor modifications, a method reported in the literature [31] was followed to prepare the spherical ZnO-NPs. In brief, 0.225 M $Zn(CH_3COO)_2 \cdot 2H_2O$ was made in 40 mL methanol and refluxed for 30 min, and then, 5 mL DDW was added. Afterward, 0.6 M NaOH in 30 mL methanol was introduced drop by drop and the refluxing was further continued at 60 °C for another 30 min. The mixture was centrifuged to collect the precipitate, repeatedly washed with a mixture of acetone in ethanol (50%, *v/v*), and dried in an air-circulating oven overnight.

Preparation of coffee residue and magnetic coffee residue

The coffee residue (CR) was collected from selected cafeterias and local coffee markets at Haramaya University and processed as follows. The collected CR was repeatedly washed with hot water, left to dry in the air for 8 h, and oven-dried for a day at 50 °C. The processed CR was repeatedly washed with DDW to get rid of any soluble dirtiness and colored components, and oven dried at 105 °C. The dehydrated CR was crushed using an electric coffee grinder and sieved into about 300–400 µm sieves to obtain a homogeneous particle size. Then, the processed CR was kept in an air-tight container for further use.

The MCR was prepared in the course of Fe(III) and Fe(II) chemical co-precipitation in the existence of CR [32]. Briefly, 1 g of the processed CR was completely dispersed in 40 mL DDW and then, 0.85 g $FeCl_3 \cdot 6H_2O$ and 0.23 g $FeCl_2 \cdot 4H_2O$ were added. While stirring vigorously (1000 rpm), the mixture was heated to 80 °C for 30 min in a nitrogen atmosphere. After the addition of 25 *wt*% ammonia solution (2 mL), the solution was kept undisturbed until the precipitation process was completed. Using an external magnet obtained from K&J Magnetics, Inc. (Pipersville, Pennsylvania, USA) (0.66 T, 10 x 10 x 0.5 cm), the precipitate was collected, repeatedly washed, and dried in a vacuum at 65 °C. Finally, it was finely ground with mortar and pestle and stored in a sealed urn.

Characterization

X-ray diffraction (XRD) analysis of the primary crystallite materials was carried out with an X'pert PRO diffractometer (PANalytical). The average crystallite sizes of the ZnO-NPs were estimated from the strongest diffraction peak using the Debye-Scherrer equation (Equation 1) [33].

$$D = \frac{k\lambda}{\beta cos\theta} \tag{1}$$

where D is the mean size of the ordered domains (nm), k is the dimensionless shape factor (typical value, 0.9), λ is the X-ray wavelength ($\lambda = 1.5405$ Å), β the line broadening (radians) and θ is the Bragg angle (degrees).

Morphology and particle size distribution of the solids were investigated by SEM (Hitachi H-7500, Tokyo, Japan) with a voltage of 10 kV. The size of the ZnO-NPs was estimated from the SEM images using Nano Measurer software. The infrared spectra of the as-synthesized materials were determined using an FTIR spectrometer (Spectrum 65 FT-IR, PerkinElmer, USA) at room temperature from the vibrational infrared spectra extending in the range of 400–4000 cm^{-1}. Appropriate amounts of the materials were ground and mixed with KBr and the percent transmittance of the materials was read and recorded. For the characteristic absorption maximum estimation of ZnO-NPs, samples dispersed in DDW were measured by UV-Vis spectrophotometer (Shimadzu UV-3600, Kyoto, Japan) using a quartz cuvette by scanning over 200–600 nm wavelength range. The materials' Zeta potential (ζ-potential) and hydrodynamic size were measured by Nano Zetasizer obtained from Malvern Instruments (Worcestershire, UK).

Determination of zinc ions

The quantification measurements of zinc ion in the NPs solution were carried out using FAAS, Perkin Elmer Analyst 700 (Waltham, MA, USA) with flame, an air-acetylene gas composition, and a zinc hollow-cathode lamp at a wavelength of 213.9 nm. The instrument was run according to the manufacturer's recommendations. To determine the Zn content of ZnO-NPs, the required amount of the pristine NPs was dispersed in DDW by sonication (30 min) to obtain its stock suspensions in the first place. To learn the actual amount of ZnO-NPs in the standard suspensions, measured volume of the suspension was centrifuged (rpm, 14,000 for 30 min) [19] and the sediment was digested with a mixed solution of HNO_3 (2 mL) and H_2O_2 (1 mL). The digested aliquot was diluted and analyzed by FAAS and the concentration of the NPs was calculated using external calibration curves. The liquid portion after centrifugation was also analyzed to learn the extent of the NPs dissolution [19]. The free Zn^{2+} concentration in ZnO-NPs suspensions was considered from the difference of initial (C_i) and final concentration (C_f) of Zn ion in the sample solution.

MSPE procedure

The MSPE was performed according to the following procedure. To 10 mL of water sample spiked with 50 mg L^{-1} ZnO-NP, 75 mg MCR was added and the mixture was agitated for 120 min. The resulting ZnO-NPs loaded MCR was collected by an external magnet, re-dispersed in 4 mL of 0.001 M HCl solution, and shaken for 30 min for desorption. After separation, known volume of the solution was withdrawn and diluted to an appropriate volume for FAAS analysis. The whole procedure involving the synthesis of MCR and the developed MSPE is schematically shown in Figure 1.
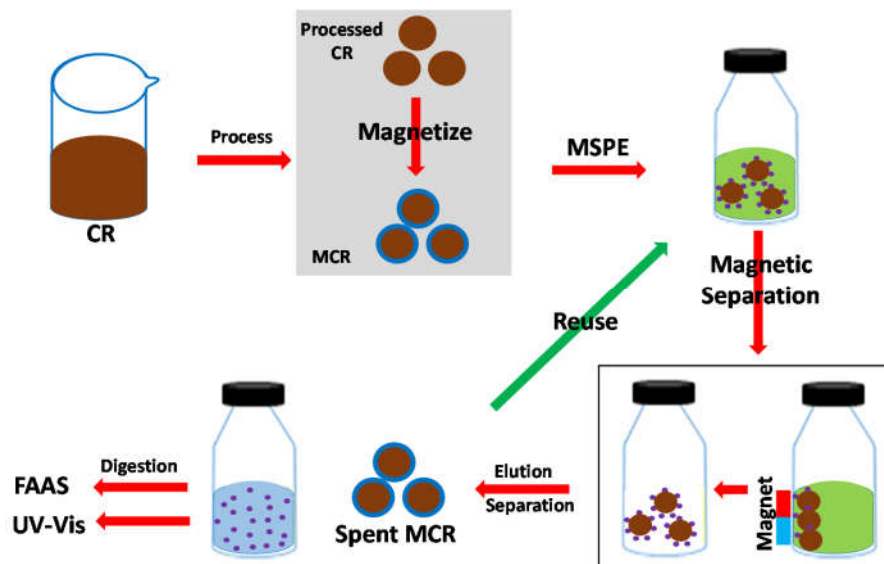

Figure 1. Schematic representation of magnetic coffee residue preparation and magnetic solid phase extraction of ZnO-NPs.

Sample collection

Three water samples, river, tap, and effluent, were collected and analyzed to assess the practical usability of the proposed technique on real-world water samples. The river water was collected from the river of Dawee located in Kurfaa Challe Woreda, Eastern Harerghe Zone of the Oromia Regional State, Ethiopia. Effluent samples were collected from Haramaya University, Haramaya Town, and Harar Brewery Share Company located in Harar Town, Ethiopia, and the tap water was sampled from Haramaya University, Haramaya, Ethiopia.

RESULTS AND DISCUSSION

Characterization

Characterization of CR and MCR. Diffraction patterns of CR and MCR are shown in Figure 2a and the results revealed that diffractograms of the materials are characterized by the presence of well-defined Bragg peaks. In the diffractogram of CR broad peaks are observed at two points ($2\theta \approx 15.6°$ and $21.5°$), which might be due to the comprised cellulosic compounds in the CR but on the antagonistic side hemicelluloses, and other ingredients of CR possess an amorphous structure [34]. On the other hand, along with the peaks detected in the pattern of CR, the MCR diffractogram showed the most prominent peaks corresponding to reflections from the planes (211), (220), (311), (400), (422), (511), (440) and (533) of magnetite [35]. Furthermore, since the observed peaks in the diffraction pattern of CR are also observed in that of MCR, although the peak intensity is weak due to the magnetite coating, it can be said that the synthesis of MCR from CR was successful.

SEM analyses were performed to learn the morphology of CR and MCR, and the corresponding images are presented in Figure 2b and Figure 2c, respectively. The micrograph shows that CR has a scraggy surface with heterogeneous holes (Figure 2b), and a comparable micrograph was reported [36]. The MCR also exhibited an analogous morphological feature with CR (Figure 2c), with a more porous and irregular structure [37] resulting in high surface area and hence, a good candidate for adsorption purposes. The MCR images also showed that the CR surface is covered by spherical magnetic iron oxide NPs which indicates that Fe_3O_4-NPs are homogeneously and uniformly ornamented forming a cage-like structure [38-40].

To study the available functional groups in the materials, and to understand the interaction mechanism of the adsorbent with the target analyte, FTIR analysis was made and the results are provided. As shown in Figure 2d, the key representative bands in FTIR spectra of CR and MCR are comparable although there are certain IR peaks observed which are recognized to different functional groups. The absorption bands at 3414, 2935, and 2849 cm^{-1} are due to the stretching vibration of hydroxyl (O-H) groups, C-H asymmetric and symmetric stretching of methyl (-CH_3) and methylene (-CH_2-) groups from the cellulose, respectively. The strong band at 1744 cm^{-1} and 1647 cm^{-1} could be due to the characteristic stretching vibration of C=O and C=C, respectively. The band at 1040 cm^{-1} indicates stretching vibration of C-N bonds of the caffeine [34, 41]. In addition, the stretching vibration of the Fe-O on the surface of the magnetite is observed at 580 cm^{-1} [35]. The IR bands of MCR after extraction of ZnO-NPs (indicated as Aft MCR in Figure 2d) become enlarged and the new peak around 446 cm^{-1} which can be assigned to Zn-O stretching vibration indicates the adsorption of ZnO-NPs on the adsorbent surface, and further, the characteristic IR band of Fe-O was shifted from 580 cm^{-1} to 588 cm^{-1}. Generally, FTIR characterization results indicated that the MCR was successfully synthesized and the magnetite NPs were deposited on the surface of CR without affecting its structural properties [37].

According to the dynamic light scattering (DLS) analysis of the CR and MCR, the hydrodynamic sizes were 3849.7 and 4223.6 nm, respectively (Table 1) which simply shows that magnetizing the processed CR increases its size due to the deposition of Fe_3O_4-NPs on the CR

surface. ζ- Potentials of CR, MCR, and ZnO-NPs were also analyzed to study the behavior of the dispersed materials' surface charge, and the results are presented (Table 1). The ζ- potentials of CR and MCR were obtained to be -21.9 mV and -21.8 mV, respectively, which indicates that their surfaces are negatively charged, while a ζ-potential value of +27.4 mV was obtained for ZnO-NPs indicating its positive surface charge. The results show that the NPs can interact with the MCR adsorbent *via* electrostatic interactions.
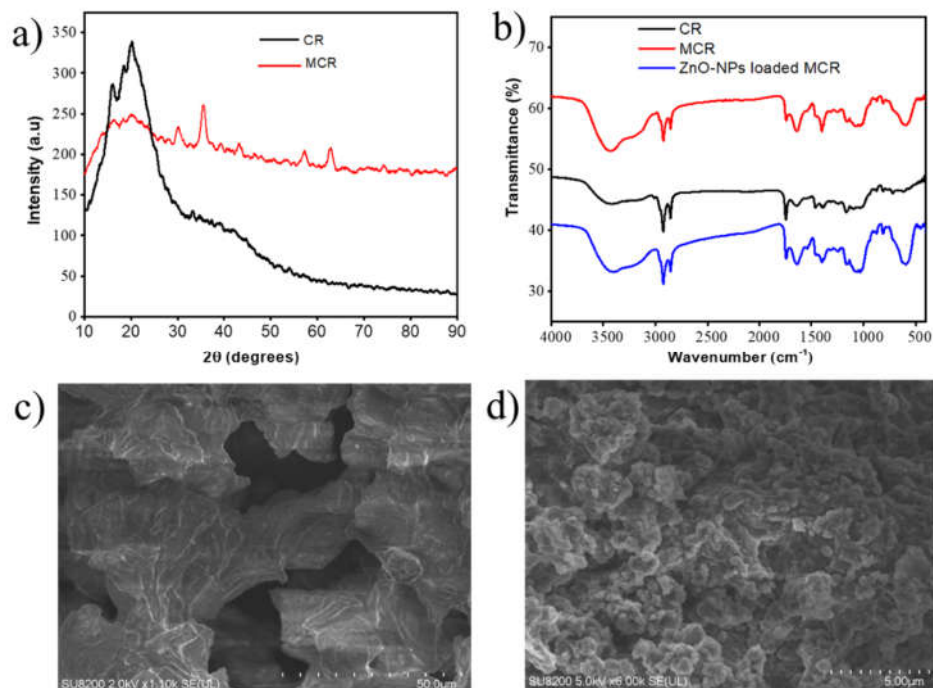

Figure 2. Characterization results of coffee residue and magnetic coffee residue. X-ray diffraction patterns of coffee residue and magnetic coffee residue (a), Fourier transform infrared spectra of coffee residue, magnetic coffee residue, and ZnO-NPs loaded magnetic coffee residue (b). Scanning electron microscopy images of coffee residue (c) and magnetic coffee residue (d).

Table 1. DLS and ζ potential analysis results of coffee residue, magnetic coffee residue, and ZnO-NPs (mean ± SD, n = 3).

Materials	Zeta potentials (mV)	DLS size (nm)
Coffee residue	−21.9 ± 0.6	3850 ± 530
Magnetic coffee residue	−21.8 ± 1.5	4220 ± 530
ZnO-NPs	+27.4 ± 2.8	186 ± 4.6

The pH drift method was used to determine the pHpzc of the adsorbent according to the following procedure. The pH of a sample solution containing 10 mM NaCl (20 mL) was adjusted in the range of 2 and 10 with diluted HCl or NaOH solutions. Then, 500 mg MCR was added and equilibrated for 24 h on a shaker. After measuring the final pH, the final pH versus the initial pH was plotted. The pH where the two curves, initial pH and final pH lines, cross each other was

considered as the pHpzc, and it is the point where the adsorbent had a neutral surface charge and is useful for explaining the adsorption mechanism [42]. When the pH of the solution is above the pHpzc, the surface charge of the adsorbent becomes negative and practically binds positively charged entities while at lower pH of the solutions than pHpzc, the surface of the adsorbent becomes positively charged and possibly captures anionic species [43]. As can be seen from Figure 3, the pHpzc of MCR is approximately 3.7, which is comparable with the literature data [36]. This indicates that the MCR can best interact with ZnO-NPs above pH of 3.7 because the surface of the MCR is negative above pHpzc and hence, the NPs can easily interact with the adsorbent. Furthermore, the pHpzc value is similar to that of the zeta potential of the adsorbent which was found to be negative (Table 1) and that of ZnO-NPs was positive, which results in reasonable interaction and hence, good extraction efficiency could be expected.
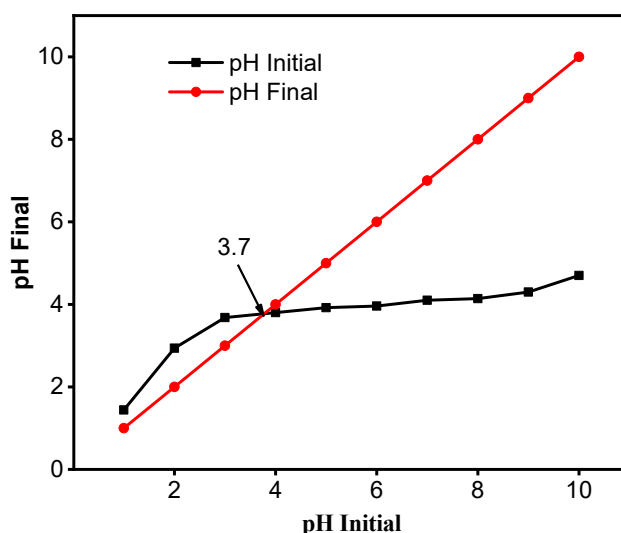
Figure 3. pHpzc curve of the magnetic coffee residue.

Characterization of ZnO-NPs

According to SEM images of the NPs (Figure 4a), the particles have a spherical morphology and are almost uniform in size distribution, and the size of the NPs was estimated using Nano Measurer software (considering over 100 particles) and the average size was found to be ~27.7 nm (Figure 4b). Compared with the particle size estimated from the XRD diffraction patterns, 19.5 nm, the SEM analysis showed a larger particle size which is scientifically expected [31, 44].

The XRD analysis of ZnO-NPs was carried out and the corresponding diffraction pattern is presented (Figure 4c). The material can be indexed to the hexagonal wurtzite structure of ZnO [44]. The XRD spectra of ZnO-NPs showed peaks at 2θ of 31.85º, 34.51º, 36.33º, 47.63º, 56.58º, 62.95º and 67.9º which corresponds to Miller indices of (100), (002), (101), (012), (110), (111) and (013), respectively. Among this, the three strongest peaks at Bragg angles of 31.85º, 34.5º, and 36.33º with lattice constants of a = 3.22000 Å and c = 5.20000 Å were observed which are consistent with the standard PDF database (JCPDS file No. 96-101-1259). Besides, there was no other intense peak, which confirms the absence of impurity, and hence, the product is purely ZnO. The crystalline size of the material was estimated to be 19.5 nm from the diffraction pattern.
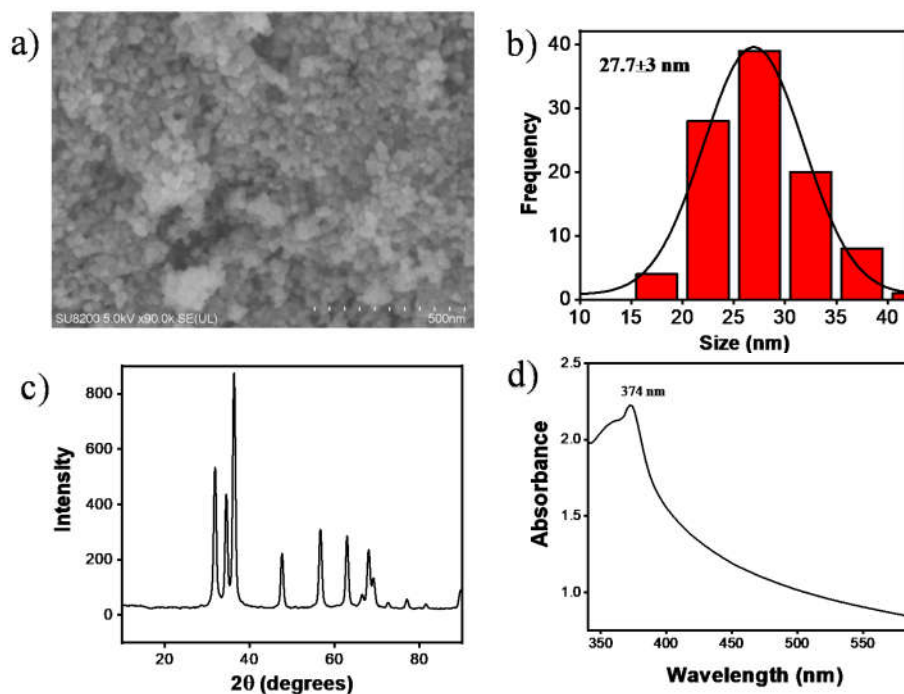
Figure 4. Characterization results of ZnO-NPs. Scanning electron microscopy images (a), size distribution histogram (b), X-ray diffraction patterns (c), and Ultraviolet-visible spectra (d).

The UV-Vis spectrum of the synthesized ZnO-NPs is presented in Figure 4d. As can be seen, the absorption maximum was observed at 374 nm, which corresponds to the characteristic λ_{max} of ZnO-NPs usually expected below 400 nm [44].

Based on the dynamic light scattering analysis, the hydrodynamic size of ZnO-NPs was found to be 185.5 nm (Table 1), which is higher than the sizes estimated from the SEM and XRD results. Such inconsistency in size could be because of that the NPs are not perfectly sphere-shaped, absence of hydration coating in the SEM analysis, and aggregation of the NPs is also likely in the solvent [31, 44].

Quantification of ZnO-NPs in the suspensions

As mentioned earlier, FAAS was employed to quantify Zn^{2+} contents in the suspensions using Zn^{2+} standard solutions. The suspension was digested before aspirating to FAAS and the analysis outcome was compared with the known concentrations. The results showed that about 2.3% of the ZnO-NPs were found to undergo dissolution during suspension (data not shown) which agrees with the literature data [19, 44]. Accordingly, the stock solution needs to be freshly prepared, and in this study, the stock suspensions were prepared at least once in two weeks which was also recommended in our previous work [44].

Optimization of the MSPE procedure

Before optimization of the extraction conditions, the affinity of the MCR towards the ZnO-NPs and desorption of the loaded analyte have been evaluated. The adsorption experiments were performed on working solutions of different concentrations and UV-Vis absorbance of the solutions before and after the adsorption process was measured and compared, and the results showed that the adsorptions capacity of MCR towards the ZnO-NPs was found to be around 93% (Table 2). For the desorption purpose, different molar concentrations of HCl and HNO_3 were investigated to select the best eluent that performs well and is compatible with the FAAS at the same time. The obtained result shows that 0.001 M HCl was found to be the best eluent and ~94% extraction efficiency (Equation 2) was obtained, accordingly.

$$\%EE = \frac{C_d}{C_i} * 100 \tag{2}$$

where %EE is the percent extraction efficiency of NPs after adsorption, C_i is the initial concentration of the NPs before adsorption; C_d is the desorbed concentration of the NPs by appropriate solvent from the surface of the MCR adsorbent [45].

Table 2. The adsorption capacity of magnetic coffee residue adsorbent (mean ± SD, n = 3).

Initial concentration (mg L^{-1})	Final concentration (mg L^{-1})	Adsorption capacity (%)
5.4	0.4	92.8 ± 1.0

After the affinity of MCR towards ZnO-NPs was learned, the optimization experiments were conducted to select optimum conditions for the MSPE procedure. The pH of the solution is among the major parameters that can affect the MSPE of ZnO-NPs. The pH effect was investigated by adjusting the pH between 5 and 10 using diluted HNO_3 and NaOH solutions, since insignificant extraction efficiency was observed below pH 5, probably due to the dissolution of ZnO-NPs. As shown in Figure 5a, as the pH increases above 5, the extraction efficiency increases but below 50% up to pH 7.5 and then, abruptly increased and attained its maximum value, ~ 93%, at pH 8.5. After that, the extraction efficiency slightly decreased, which might be caused by the OH- effect on the ZnO-NPs surface charge. Therefore, the sample solution pH value of 8.5 was considered in subsequent experiments.

The influence of the adsorbent amount was investigated at optimal pH by varying the adsorbent amount in the range of 25–150 mg keeping other parameters unaltered. The results (Figure 5b) depicted the presence of a rapid increase in the extraction efficiency with increasing adsorbent dosage up to 75 mg due to the availability of more adsorption sites [46]. But, a trivial change in the extraction efficiency was observed above 75 mg (Figure 5b). In general, since 75 mg MCR adequately extracts the ZnO-NPs (extraction efficiency, ~ 93%), it was considered to be the optimum amount.

The effect of the sample volume was investigated in the range of 5–100 mL for the extraction of 50 mg L^{-1} of ZnO-NPs to study the ability of the proposed technique in the preconcentration of trace amounts of ZnO-NPs. According to the results, the highest extraction performance was obtained when a 10 mL sample solution was considered and then reduced as the sample volume further increased (Figure 5c). When the sample volume increased above 10 mL at the optimum adsorbent dose, the extraction efficiency decreased since the amount of analyte also increase, so limited adsorption sites are present. Thus, 10 mL was selected as an optimum sample volume.

Extraction time is another important parameter that has to be optimized. MSPE is an equilibrium process in which adequate time is required for the extraction procedure to guarantee ample adsorption of the analytes on the adsorbent surface. Accordingly, various extraction times (5–180 min) were examined and the time required to achieve equilibrium beyond which no more ZnO-NPs were further removed from the suspension was identified. As depicted in Figure 5d, the

maximum extraction efficiency of the analyte was obtained in 120 min and considered as an optimum extraction time in the following experiments.
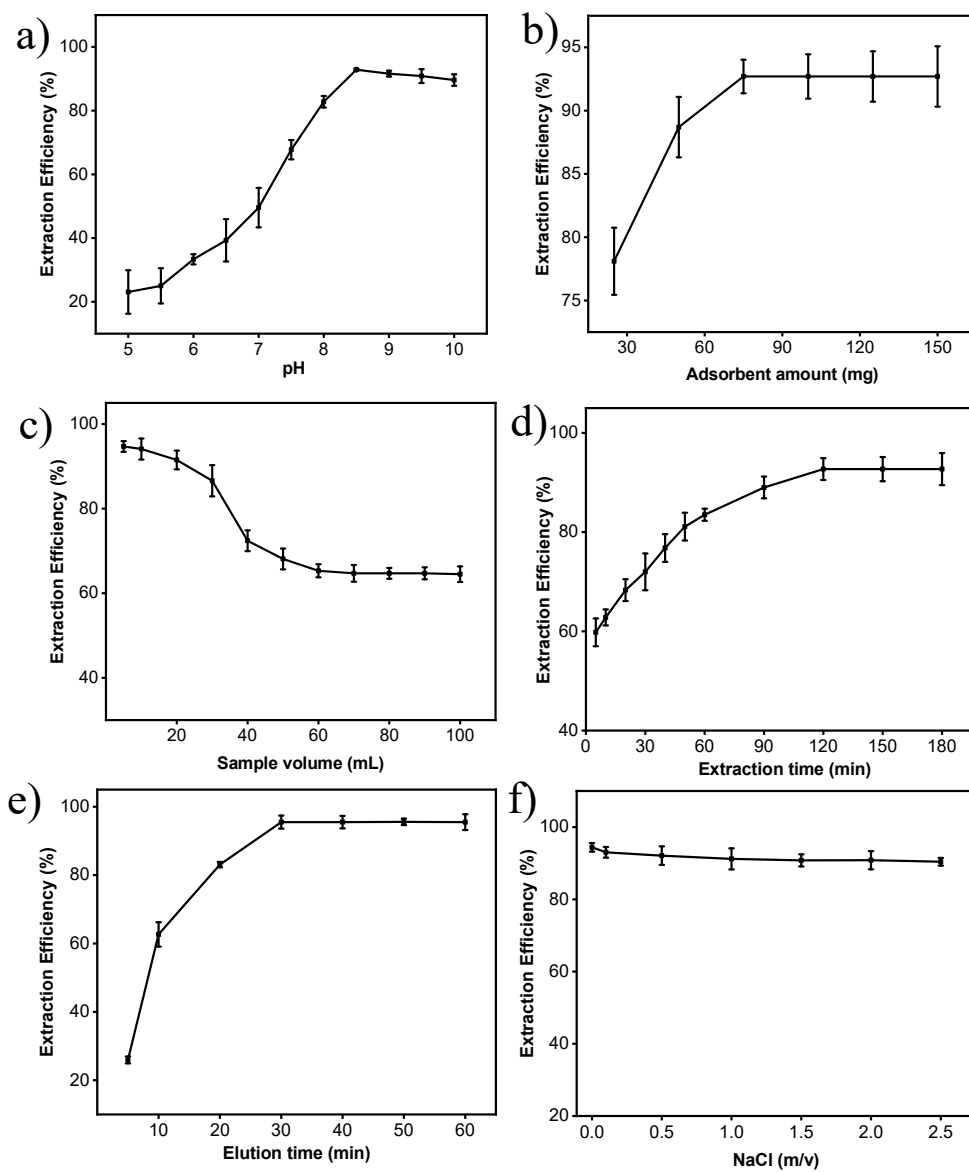

Figure 5. Effects of pH (a), adsorbent dosage (b), sample volume (c), extraction time (d), elution time (e), and ionic strength (f) on the magnetic solid-phase extraction of ZnO-NPs.

The desorbing solvent has to quantitatively recover the target analyte within the optimum time and should be also compatible with the instruments. Different concentrations of HNO_3 and HCl were examined to determine a suitable desorbing solution. It was found that 4 mL of 0.001 M HCl quantitatively desorbed ZnO-NPs from the surface of the MCR. After selecting the best type and volume of eluent, the influence of elution time was also evaluated, and 95% of ZnO-NPs were found to be quantitatively desorbed within 30 min (Figure 5e). Consequently, 4 mL of 0.001 M HCl with an elution time of 30 min was taken as optimum elution conditions.

The effect of the sample ionic strength was also investigated with different NaCl concentrations in the range of 0.1–2.5% (*m/v*) [44] and changes in the ionic strength were found to affect the extraction efficiency, insignificantly (Figure 5f). This observation indicates the possible applicability of the developed procedure for the extraction and enrichment of ZnO-NPs in salty water samples such as seawater. Therefore, no salt addition was made in further experiments.

Selectivity

The selectivity of MCR towards ZnO-NPs in the presence of Zn^{2+} was first studied by considering the capacity of MCR to adsorb Zn^{2+}. As a result, the interference of zinc ion species on the extraction of ZnO-NPs was investigated by spiking different concentrations of Zn^{2+} (0–6 mg L^{-1}) to 6 mg L^{-1} ZnO-NPs. The results revealed that the minimal adsorption capacity of the adsorbent towards Zn^{2+}, less than 5%, was observed at optimum conditions. This indicates that extraction of Zn^{2+} ion by MCR is negligible compared to ZnO-NPs but, the very slight variation in adsorption efficiency might be due to co-adsorption of the Zn^{2+} ion. Rather in the presence of ZnO-NPs, Zn^{2+} ion may be correspondingly co-adsorbed giving slightly visible adsorption efficiency of the analyte. Figure 6a clearly shows that the extraction capacity of ZnO-NPs in the presence of Zn^{2+} ion was not affected and an almost constant result was obtained. Generally, the above conditions indicate a profound selectivity of MCR towards ZnO-NPs over Zn^{2+} and thus, the proposed method has an outstanding potential to selectively extract ZnO-NPs even from aqueous suspensions containing Zn^{2+} ions.
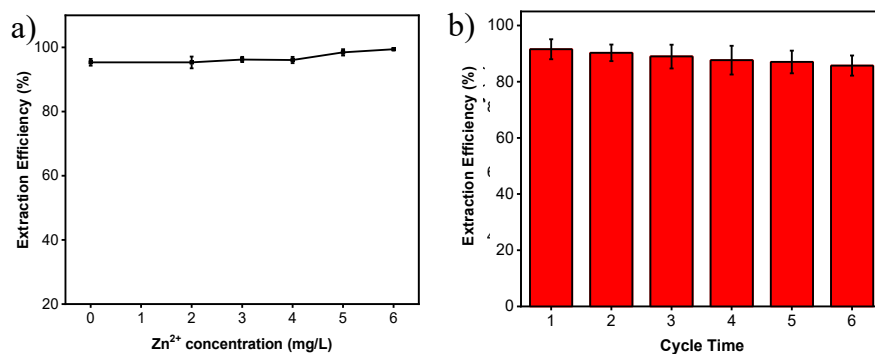

Figure 6. Effect of Zn^{2+} on the magnetic solid-phase extraction of ZnO-NPs (a) and reusability of the magnetic coffee residue (b).

Reusability of MCR

Recyclability is among the parameters that evaluate adsorbent qualities and is required from the green analytical chemistry point of view. To this end, the reusability and stability of the MCR

were evaluated at the optimum environments based on its performance after six consecutive cycles. After desorption, the spent adsorbent was recovered by the external magnetic field, washed with DDW to remove residual acid, dried, and used for the next adsorption. The outcomes displayed that the MCR is firm and recyclable with insignificant loss in adsorption ability and a slight drop in the extraction efficiency of the considered NPs with variations less than 5% were observed during the consecutive extraction processes (Figure 6b). But this slight change in extraction efficiency might be due to inaccuracy associated with restoration and cleansing processes.

Analytical performances

Under the optimum circumstances, the analytical performances of the developed technique were convincing for the quantification of ZnO-NPs. As shown in Table 3, the method exhibited strong linearity (R^2 = 0.994) in the concentration range between 0.25 and 8.0 mg L^{-1}. The limit of detection (LOD) and limit of quantification (LOQ) of the developed method (elucidated as LOD = 3*s and LOQ = 10*s (n = 8), where s is the standard deviation of the measurements) was obtained to be 0.12 and 0.4 mg L^{-1}, respectively, and the intra-day and inter-day relative standard deviations (RSD) at 6 mg L^{-1} of ZnO-NPs were obtained to be 1.4 and 2.2%, respectively.

Table 3. Analytical performance of the proposed method at the optimized conditions.

Parameters	Results
Linear range (mg L^{-1})	0.25–8.0
Correlation coefficient (R^2)	0.994
LOD (mg L^{-1})	0.12
LOQ (mg L^{-1})	0.4
Intra-day RSD (%)	1.4
Inter-day RSD (%)	2.2

Application on environmental waters

The practical applicability of the proposed extraction procedure for the analysis of ZnO-NPs in complex matrices such as environmental water samples (river, tap, and effluent) was evaluated. The river and effluent water samples were filtered before analysis. Before the spiking experiment, the concentration of ZnO-NPs in the environmental samples was assayed and found to be below the LOD for all samples. As shown in Table 4, the % recovery values of ZnO-NPs from the fortified samples were between 93.0 and 98.2%, which indicates that the developed technique is capable of determining trace ZnO-NPs in real-world water samples.

Table 4. The extraction efficiency of ZnO-NPs in environmental waters by using the proposed method, (mean ± SD, n = 3).

Sample	Spiked (mg L^{-1})	Detected (mg L^{-1})	Extraction efficiency (%)
River	1	0.93 ± 0.2	93.0
	5	4.70 ± 0.4	93.8
Haramaya University Effluent	1	0.97 ± 0.3	96.4
	5	4.80 ± 0.2	97.0
Harar Beer Factory Effluent	1	0.95 ± 0.2	94.4
	5	4.70 ± 0.2	95.0
Tap	1	0.94 ± 0.2	94.0
	5	4.90 ± 0.4	98.2

CONCLUSION

MCR adsorbent was successfully prepared by co-precipitation of the CR with Fe_3O_4-NPs and used as a potential adsorbent for the extraction and preconcentration of trace ZnO-NPs from water samples. The prepared NPs and adsorbent were characterized by numerous methods including UV-Vis, XRD, SEM, FTIR, and DLS. The separation, enrichment, and quantification of ZnO-NPs from a complex aqueous medium in the presence of its corresponding ion were carried out with the developed MSPE under optimized conditions. Moreover, the proposed method allows easy and rapid separation of the analyte, ZnO-NPs, using an external magnetic field and was successfully applied for the extractions of ZnO-NPs from different environmental water samples (river, effluents, and tap water). In general, the technique is simple, environmentally friendly, and cost-effective and hence, recommended for the analysis of metal oxide NPs from various types of waters.

ACKNOWLEDGMENTS

REFERENCES

1. Piccinno, F.; Gottschalk, F.; Seeger, S.; Nowack, B. Industrial production quantities and uses of ten engineered nanomaterials in Europe and the world. *J. Nanopart. Res.* **2012**, 14, 1109.
2. Nakayama, Y.; Pauzauskie, P.J.; Radenovic, A.; Onorato, R.M.; Saykally, R.J.; Liphardt, J.; Yang, P. Tunable nanowire nonlinear optical probe. *Nature* **2007**, 447, 1098–1101.
3. Amde, M.; Tan, Z.Q.; Liu, R.; Liu, J.F. Nanofluid of zinc oxide nanoparticles in ionic liquid for single drop liquid microextraction of fungicides in environmental waters prior to high performance liquid chromatographic analysis. *J. Chromatogr. A* **2015**, 1395, 7–15.
4. Amde, M.; Liu, J.-F.; Tan, Z.-Q.; Bekana, D. Ionic liquid-based zinc oxide nanofluid for vortex assisted liquid liquid microextraction of inorganic mercury in environmental waters prior to cold vapor atomic fluorescence spectroscopic detection. *Talanta* **2016**, 149, 341–346.
5. Hossain, M.F.; Takahashi, T.; Biswas, S. Nano-rods and nano-lipsticks structured ZnO photo-electrode for dye-sensitized solar cells. *Electrochem. Commun.* **2009**, 11, 1756–1759.
6. Li, Y.; Wu, K.; Zhitomirsky, I. Electrodeposition of composite zinc oxide–chitosan films. *Colloids Surf. A: Physicochem. Eng. Asp.* **2010**, 356, 63–70.
7. Singh, J.; Im, J.; Whitten, J.E.; Soares, J.W.; Steeves, D.M. Chemisorption of a thiol-functionalized ruthenium dye on zinc oxide nanoparticles: Implications for dye-sensitized solar cells. *Chem. Phys. Lett.* **2010**, 497, 196–199.
8. Xiang, C.; Zou, Y.; Sun, L.-X.; Xu, F. Direct electrochemistry and enhanced electrocatalysis of horseradish peroxidase based on flowerlike ZnO–gold nanoparticle–Nafion nanocomposite. *Sens. Actuators B Chem.* **2009**, 136, 158–162.
9. Zhao, J.; Zhi, J.; Zhou, Y.; Yan, W. A tyrosinase biosensor based on ZnO nano-rod clusters/nano-crystalline diamond electrodes for bio-sensing of phenolic compounds. *Anal. Sci.* **2009**, 25, 1083–1088.
10. Padmavathy, N.; Vijayaraghavan, R. Enhanced bioactivity of ZnO nanoparticles — an antimicrobial study. *Sci. Technol. Adv. Mater.*, **2008**, 9, 035004.
11. Ansari, S.A.; Husain, Q.; Qayyum, S.; Azam, A. Designing and surface modification of zinc oxide nanoparticles for biomedical applications. *Food Chem. Toxicol.* **2011**, 49, 2107–2115.
12. He, L.; Liu, Y.; Mustapha, A.; Lin, M. Antifungal activity of zinc oxide nanoparticles against *Botrytis cinerea* and *Penicillium expansum*. *Microbiol. Res.* **2011**, 166, 207–215.

13. Feng, J.N.; Guo, X.P.; Chen, Y.R.; Lu, D.P.; Niu, Z.S.; Tou, F.Y.; Hou, L.J.; Xu, J.; Liu, M.; Yang, Y. Time-dependent effects of ZnO nanoparticles on bacteria in an estuarine aquatic environment. *Sci. Total Environ.* **2020**, 698, 134298.

14. Rajput, V.; Minkina, T.; Sushkova, S.; Behal, A.; Maksimov, A.; Blicharska, E.; Ghazaryan, K.; Movsesyan, H.; Barsova, N. ZnO and CuO nanoparticles: a threat to soil organisms, plants, and human health. *Environ. Geochem. Health*, **2020**, 42, 147–158.

15. Amde, M.; Liu, J.; Tan, Z.-Q.; Bekana, D. Transformation and bioavailability of metal oxide nanoparticles in aquatic and terrestrial environments. A review. *Environ. Pollut.* **2017**, 230, 250–267.

16. Zhou, Q.; Liu, L.; Liu, N.; He, B.; Hu, L.; Wang, L. Determination and characterization of metal nanoparticles in clams and oysters. *Ecotoxicol. Environ. Saf.* **2020**, 198, 110670.

17. Liu, J.F.; Chao, J.B.; Liu, R.; Tan, Z.Q.; Yin, Y.G.; Wu, Y.; Jiang, G.B. Cloud point extraction as an advantageous preconcentration approach for analysis of trace silver nanoparticles in environmental waters. *Anal. Chem.* **2009**, 81, 6496–6502.

18. Chao, J.B.; Liu, J.F.; Yu, S.J.; Feng, Y.D.; Tan, Z.Q.; Liu, R.; Yin, Y.G. Speciation analysis of silver nanoparticles and silver ions in antibacterial products and environmental waters via cloud point extraction-based separation. *Anal. Chem.* **2011**, 83, 6875–6882.

19. Majedi, S.M.; Lee, H.K.; Kelly, B.C. Chemometric analytical approach for the cloud point extraction and inductively coupled plasma mass spectrometric determination of zinc oxide nanoparticles in water samples. *Anal. Chem.*, **2012**, 84, 6546–6552.

20. Li, L.; Leopold, K. Ligand-assisted extraction for separation and preconcentration of gold nanoparticles from waters. *Anal. Chem.* **2012**, 84, 4340–4349.

21. Li, L.; Leopold, K.; Schuster, M. Effective and selective extraction of noble metal nanoparticles from environmental water through a noncovalent reversible reaction on an ionic exchange resin. *Chem. Commun.* **2012**, 48, 9165–9167.

22. Giakisikli, G.; Anthemidis, A.N. Magnetic materials as sorbents for metal/metalloid preconcentration and/or separation. A review. *Anal. Chim. Acta* **2013**, 789, 1–16.

23. Xu, J.; Zheng, J.; Tian, J.; Zhu, F.; Zeng, F.; Su, C.; Ouyang, G. New materials in solid-phase microextraction. *Trends Anal. Chem.* **2013**, 47, 68–83.

24. Basu, M.; Guha, A.K.; Ray, L. Biosorptive removal of lead by lentil husk. *J. Environ. Chem. Eng.* **2015**, 3, 1088–1095.

25. Bailey, S.E.; Olin, T.J.; Bricka, R.M.; Adrian, D.D. A review of potentially low-cost sorbents for heavy metals. *Water Res.* **1999**, 33, 2469–2479.

26. Bagbi, Y.; Sarswat, A.; Mohan, D.; Pandey, A.; Solanki, P.R. Lead (Pb^{2+}) adsorption by monodispersed magnetite nanoparticles: Surface analysis and effects of solution chemistry. *J. Environ. Chem. Eng.* **2016**, 4, 4237–4247.

27. Li, Q.; Zhan, Z.; Jin, S.; Tan, B. Wettable magnetic hypercrosslinked microporous nanoparticle as an efficient adsorbent for water treatment. *Chem. Eng. J.* **2017**, 326, 109–116.

28. Safarik, I.; Horska, K.; Svobodova, B.; Safarikova, M. Magnetically modified spent coffee grounds for dyes removal. *Eur. Food Res. Technol.* **2011**, 234, 345–350.

29. Zuorro, A.; Lavecchia, R. Removal of Methylene Blue from Aqueous Solution by Adsorption on Low-Grade Green Coffee Beans. *Adv. Mater. Res.* **2013**, 800, 72–76.

30. Firomesa, H.; Amde, M.; Bekana, D.; Temesgen, A. Magnetic coffee residue as sorbent for magnetic solid-phase extraction and determination of titanium dioxide nanoparticles in water samples. *Chem. Pap.* **2022**, 76, 2267–2277.

31. Wu, C.-M.; Baltrusaitis, J.; Gillan, E.G.; Grassian, V.H. Sulfur Dioxide Adsorption on ZnO Nanoparticles and Nanorods. *J. Phys. Chem. C* **2011**, 115, 10164–10172.

32. Kazemi, E.; Dadfarnia, S.; Shabani, A.M.H. Dispersive solid phase microextraction with magnetic graphene oxide as the sorbent for separation and preconcentration of ultra-trace amounts of gold ions. *Talanta*, **2015**, 141, 273–278.

33. Chen, C.; Liu, P.; Lu, C. Synthesis and characterization of nano sized ZnO powders by direct precipitation method. *Chem. Eng. J.* **2008**, 144, 509–513.
34. Ballesteros, L.F.; Teixeira, J.A.; Mussatto, S.I. Chemical, functional, and structural properties of spent coffee grounds and coffee silverskin. *Food Bioprocess Technol.* **2014**, 7, 3493–3503.
35. Petcharoen, K.; Sirivat, A. Synthesis and characterization of magnetite nanoparticles via the chemical co-precipitation method. *Mater. Sci. Eng.: B* **2012**, 177, 421–427.
36. Kyzas, G.Z. Commercial coffee wastes as materials for adsorption of heavy metals from aqueous solutions. *Materials*, **2012**, 5, 1826–1840.
37. Zuorro, A.; Lavecchia, R.; Natali, S. Magnetically modified agro-industrial wastes as efficient and easily recoverable adsorbents for water treatment. *Chem. Eng. Trans.* **2014**, 38, 349–354.
38. Mosiniewicz-Szablewska, E.; Safarikova, M.; Safarik, I. Magnetic studies of ferrofluid-modified spruce sawdust. *J. Phys. D: Appl. Phys.* **2007**, 40, 6490–6496.
39. Panneerselvam, P.; Morad, N.; Tan, K.A. Magnetic nanoparticle (Fe3O4) impregnated onto tea waste for the removal of nickel(II) from aqueous solution. *J Hazard. Mater.* **2011**, 186, 160–168.
40. Safarik, I.; Lunackova, P.; Mosiniewicz-Szablewska, E.; Weyda, F.; Safarikova, M. Adsorption of water-soluble organic dyes on ferrofluid-modified sawdust. *Holzforschung* **2007**, 61, 247–253.
41. Reis, N.; Franca, A.S.; Oliveira, L.S. Discrimination between roasted coffee, roasted corn and coffee husks by Diffuse Reflectance Infrared Fourier Transform Spectroscopy. *LWT--Food Sci. Technol.* **2013**, 50, 715–722.
42. Fiol, N.; Villaescusa, I. Determination of sorbent point zero charge: Usefulness in sorption studies. *Environ. Chem. Lett.* **2009**, 7, 79–84.
43. Morin-Crini, N.; Loiacono, S.; Placet, V.; Torri, G.; Bradu, C.; Kostić, M.; Cosentino, C.; Chanet, G.; Martel, B.; Lichtfouse, E.; Crini, G. *Green adsorbents for pollutant removal* in *Environmental Chemistry for a Sustainable*, World ed., Crini, G.; Lichtfouse, E.. (Eds.), Springer, Cham: Switzerland; **2018**.
44. Amde, M.; Tan, Z.-Q.; Liu, J. Separation and size characterization of zinc oxide nanoparticles in environmental waters using asymmetrical flow field-flow fractionation. *Talanta* **2019**, 200, 357–365.
45. Johnson, W.M.; Kido Soule, M.C.; Kujawinski, E.B. Extraction efficiency and quantification of dissolved metabolites in targeted marine metabolomics. *Limnol. Oceanogr.: Methods* **2017**, 15, 417–428.
46. Tan, I.A.; Ahmad, A.L.; Hameed, B.H. Adsorption of basic dye on high-surface-area activated carbon prepared from coconut husk: equilibrium, kinetic and thermodynamic studies. *J. Hazard. Mater.* **2008**, 154, 337–346.